Lifetimes and time scales in atmospheric chemistry

By Michael J. Prather*

Earth System Science Department, University of California, Irvine, CA 92697-3100, USA

Atmospheric composition is controlled by the emission, photochemistry and transport of many trace gases. Understanding the time scale as well as the chemical and spatial patterns of perturbations to trace gases is needed to evaluate possible environmental damage (e.g. stratospheric ozone depletion or climate change) caused by anthropogenic emissions. This paper reviews lessons learned from treating global atmospheric chemistry as a linearized system and analysing it in terms of eigenvalues.

The results give insight into how emissions of one trace species cause perturbations to another and how transport and chemistry can alter the time scale of the overall perturbation. Further, the eigenvectors describe the fundamental chemical modes, or patterns, of the atmosphere's chemical response to perturbations.

Keywords: atmospheric chemistry; time scales; lifetimes; chemical modes; eigenvalues

1. Introduction to time scales

Knowledge of time scales in the Earth system has both scientific and practical applications. Chemical feedbacks in the atmosphere, for example, have been shown to extend the duration of methane perturbations (Prather 1994), thus increasing the climate impact of (and the Kyoto tax on) emissions of this greenhouse gas by 40% (IPCC 1996). Emissions of trace gases with lifetimes of a day, such as nitrogen oxides, are now predicted to perturb other greenhouse gases for decades (Derwent *et al.* 2001; Wild *et al.* 2001). Stratospheric aerosols from major volcanic eruptions mostly disappear from the atmosphere in a couple of years, yet we see decadal dips in global mean sea level resulting from their brief cooling of the Earth (Church *et al.* 2005). This paper summarizes a methodology developed over the last decade for analysing atmospheric chemistry through linearization and eigenvalue analysis. This new formalism accounts for the chemical feedbacks, describes the long temporal response to apparently short-lived perturbations, integrates over the environmental impacts of trace gas emissions, but requires us to replace our traditional view of lifetimes in atmospheric chemistry.

*mprather@uci.edu

A typical trace gas that mixes throughout the atmosphere and into the ocean and terrestrial biosphere encounters a wide range of biogeochemical conditions, each with a different reactivity. Integrating the global loss of a trace gas (L, kg yr^{-1}) and dividing it into the global burden (B, kg) of the gas yield a single number with units of time (T, yr), which has been called the lifetime or residence time (Bolin & Rodhe 1973; O'Neill *et al.* 1994). When the global source (S, kg yr^{-1}) equals the loss over a year, the trace gas is in steady state, and the lifetime ($T_{SS} = B/L = B/S$) is often thought of as a constant for the current atmosphere, a universal value that defines properties such as atmospheric variability (Junge 1974). Such lifetimes are used to provide a time scale for environmental impacts, including ozone depletion and global warming potentials (ODP and GWP). While this calculated lifetime has units of time, it is most often not a true time scale of the system and, for gases with short lifetimes, fails to identify the long duration of some impacts.

This paper develops the concept of atmospheric chemistry as a coupled system across different trace species with transport between different regions and radiative feedbacks. These three processes, individually or together, lead automatically to the new expectation that a perturbation to one species in one location will invoke a global response on a wide range of time scales, probably involving other chemical species.

The eigenvalue decomposition of a properly discretized and linearized chemistry–transport system produces eigenvectors that are perturbation patterns of trace gas abundances, also known as chemical modes. The negative inverse of the eigenvalue of each chemical mode is the time scale for the mode to decay by a factor of e. The derivation of these and related properties is presented in §2. Simple one-box examples for stratospheric ozone and tropospheric methane are given in §§3 and 4, respectively. Section 5 shows how the time scale for methyl bromide is altered by transport exchange between the stratosphere and the troposphere. Ozone interacts with other gases through control of the transmission of solar ultraviolet, and this radiative coupling changes the time scale for nitrous oxide as shown in §6. Section 7 reviews the special role of steady-state lifetime as an integrator of environmental impacts. Continuous semi-infinite systems are considered briefly in §8. Observations of the stratospheric decay mode are presented in §9. The existence of global chemical modes in realistic three-dimensional models is discussed in §10. Future applications are addressed in §11.

2. Atmospheric chemistry: linearization, time scales and chemical modes

The continuity equation describing the instantaneous rate of change in abundance V of trace gas (n) at location (x, y, z) can be expressed as

$$\frac{\mathrm{d}V(x, y, z, n)}{\mathrm{d}t} = \mathrm{Chem}[V(x, y, z, n')] + \mathrm{Tran}[V(x', y', z', n)] + \mathrm{Rad}[V(x', y', z', n'')],$$

where the chemistry operator (Chem) couples all trace species (n') but is local, the transport operator (Tran) does not interchange species but is global (x'', y'', z'') and the radiation operator (Rad) couples the trace gas to a global distribution of a few species (n'', e.g. ozone and aerosols). Under most circumstances, the time scales of perturbations to atmospheric composition can be derived from the eigenvalues of the linearized form of this continuity equation.

Assume that V is a solution for a generic operator A, $dV/dt = A[V]$, then the continuity equation for a perturbation δV can be derived as

$$\frac{d\delta V}{dt} = \frac{d[V + dV]}{dt} - \frac{dV}{dt} = A[V + \delta V] - A[V] = J_V \cdot \delta V + \text{order}(\delta V^2),$$

where the Jacobian matrix J of the operator A is the first term in the Taylor expansion of $A[V + \delta V]$ evaluated at V, i.e. the linearized system (e.g. Prather 1996, 2002; Manning 1999). The Jacobian matrix has dimension $m \times m$, where m is the number of variables. Species are inherently discrete, and adopting a discrete spatial grid gives us a finite number of variables across (x, y, z, n). For discussion of the continuum, see §8.

If the perturbation δV is an eigenvector of J_V with eigenvalue λ, then

$$\frac{d\delta V}{dt} = J_V \cdot \delta V = \lambda \delta V,$$

and the exact solution is $\delta V(t) = \delta V(0) \exp(\lambda t)$. In general, there will be a set of m linearly independent eigenvectors E_i, each with eigenvalue λ_i (yr^{-1}). For stable systems, all λ_i must be less than or equal to zero. The inverse negative eigenvalue is the mode time ($T_i = -1/\lambda_i$) determining the e-fold of the chemical mode. The $E_i(x, y, z, n)$ are dimensionless and represent a relative pattern of trace species, both in space and across species. Any perturbation can be expressed as a unique linear combination, $\delta V(0) = \sum_{i=1:m} a_i E_i$ with an exact solution $\delta V(t) = \sum_{i=1:m} a_i E_i \exp(\lambda_i t)$. In this case, the coefficients a_i have abundance units (kg) and each E_i has a scalar mass coefficient for each species (n), defined as m_i^n that sums over the eigenvector's spatial distribution of (n). The total mass of species (n) in a perturbation can be represented by the mass operator $M^n[\delta V] = \sum_{i=1:m} a_i m_i^n$ (kg).

The recognition that any perturbation to atmospheric composition can be expressed as a sum of chemical modes, each with a fixed decay term, has several important applications (Prather 1994). First, the e-folding times T_i, rather than the budget-derived lifetime T_{SS}, are the true time scales of variability in the system. Second, the asymptotic approach to a steady state becomes a single exponential decay with the largest T_i. In practical terms, this recognition has saved large amounts of computing time, since perturbations (e.g. adjustments to a new steady state, or model response functions for inverting emission sources) can be readily and accurately extrapolated. Third, a chemical mode, in general, will couple across different species, and thus a perturbation to any species should be expected to excite all modes and respond on the full range of time scales in the system. Perturbation dynamics developed by Farrell & Ioannou (2000) has extended this approach to determining which types of perturbations produce the greatest impact on a chosen species at a chosen site.

3. Stratospheric ozone chemistry: the definition of 'odd oxygen'

In the upper stratosphere, the Chapman (1930) mechanism, which includes only atomic oxygen (O), ozone (O_3) and molecular oxygen (O_2), roughly describes the abundance of ozone. Additional reactions involving others species (e.g. HO_2, NO, Cl) are needed to accurately match the observed profile and trends. When solving the continuity equations for O and O_3, researchers recognized that O_3 perturbations behaved as an empirically defined 'odd oxygen' ($O + O_3$) rather

than independently as O and O_3. Eigenvalue decomposition of the Chapman mechanism readily derives the correct time scales and shows that odd oxygen is indeed one of the fundamental perturbation patterns of this chemical system.

The Chapman reactions, their rates and coefficients typical of 42 km altitude at mid-latitudes can be summarized as

(i) $O_2 + \text{photon} \Rightarrow O + O$ $R_1 = J_1[O_2]$ $J_1 = 1.8 \times 10^{-10} \text{ s}^{-1}$

(ii) $O + O_2(+M) \Rightarrow O_3(+M)$ $R_2 = k_2[O][O_2]$ $k_2 = 5.26 \times 10^{-17} \text{ cm}^3 \text{ s}^{-1}$

(iii) $O_3 + \text{photon} \Rightarrow O_2 + O$ $R_3 = J_3[O_3]$ $J_3 = 1.4 \times 10^{-3} \text{ s}^{-1}$

(iv) $O + O_3 \Rightarrow O_2 + O_2$ $R_4 = k_4[O][O_3]$ $k_2 = 3.0 \times 10^{-15} \text{ cm}^3 \text{ s}^{-1}$.

For this abbreviated set of reactions, the chemical rate equations for the densities of atomic oxygen, ozone and molecular oxygen are

$$\frac{d[O_3]}{dt} = R_2 - R_3 - R_4$$

$$\frac{d[O]}{dt} = 2R_1 + R_3 - R_2 - R_4$$

$$\frac{d[O_2]}{dt} = 2R_4 + R_3 - R_1 - R_2,$$

and the Jacobian elements are

$$
\begin{array}{ccc}
-J_3 - k_4[O] & +k_2[O_2] - k_4[O_3] & +k_2[O] \\
+J_3 - k_4[O] & -k_2[O_2] - k_4[O_3] & +2J_1 - k_2[O] \\
+J_3 + 2k_4[O] & -k_2[O_2] + 2k_4[O_3] & -J_1 - k_2[O].
\end{array}
$$

The steady-state solution for this example is $[O] = 1.26 \times 10^9 \text{ cm}^{-3}$, $[O_3] = 6.55 \times 10^{11} \text{ cm}^{-3}$ and $[O_2] = 1.38 \times 10^{16} \text{ cm}^{-3}$. Lifetimes in atmospheric chemistry are traditionally defined in terms of a linearized loss frequency (units of s^{-1}) or, equivalently, the ratio of abundance (e.g. number cm^{-3}) divided by a production or loss rate ($\text{cm}^{-3} \text{ s}^{-1}$). For the Chapman mechanism at 42 km, we can derive the following possible lifetimes:

$$T(O_2) \quad = \quad \frac{[O_2]}{R_1} \quad = \quad 176 \text{ yr}$$

$$T(O_3) \quad = \quad \frac{[O_3]}{(R_3 + R_4)} \quad = \quad 12 \text{ min}$$

$$T(O) \quad = \quad \frac{[O]}{(R_2 + R_4)} \quad = \quad 1.4 \text{ s}$$

$$T(O + O_3 \equiv O_X) \quad = \quad \frac{[O + O_3]}{2R_4} \quad = \quad 1.5 \text{ day}$$

$$T(\text{total O}) \quad = \quad \frac{[O + 2O_2 + 3O_3]}{0} \quad = \quad \text{infinity}.$$

Molecular oxygen photolyses with an e-fold time scale of 176 yr, ozone photolyses with a time scale of 12 min and atomic oxygen reacts with O_2 on a time scale of 1.4 s. These three time scales are the negative inverse of the diagonal elements of the Jacobian of the three continuity equations above. We can define additional time constants for total oxygen and odd oxygen. As expected, the abundance of total oxygen is constant (i.e. $d([O]+2[O_2]+3[O_3])/dt=0$) and hence has a time scale of infinity. The odd oxygen time-scale, 1.5 day, is determined by recombination of O and O_3 (R_4).
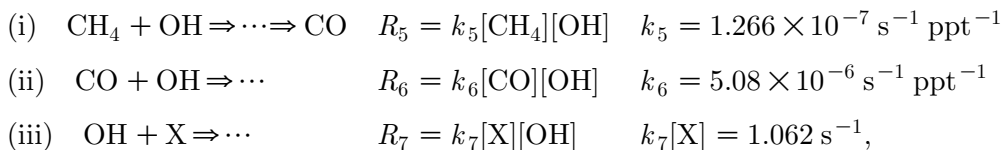
Which of these five time scales accurately describes this system? The Jacobian matrix derived from the 3×3 system of equations above has one zero eigenvalue and two non-zero eigenvalues of $-1/(1.4\,s)$ and $-1/(0.74\,day)$. The zero eigenvalue is consistent with the infinite time scale for changing total oxygen, the next larger eigenvalue is close to that for odd oxygen and the largest eigenvalue closely matches the O lifetime. The chemical mode (eigenvector) with mode time of 1.4 s is $([O_3], [O], [O_2])=(-0.995, +1.000, +0.992)$ and that with mode time of 0.74 day is $(+1.0000, +0.0019, -1.5010)$. Perturbations to the ratio $[O]:[O_3]$ disappear quickly with the time scale of O recombination (R_2), whereas those to the sum $[O]+[O_3]$ decay more slowly. This latter odd oxygen mode preserves the ratio, $[O]:[O_3]=0.0019$, of the steady-state solution.

We have lost the O_2 and O_3 time scales and have preserved only the largest eigenvalue (shortest time scale). The photolysis time for O_3 is not a time scale of this system! This is typical of coupled systems: the largest diagonal terms remain as eigenvalues, and the smaller ones are altered. The eigenvalue decomposition gives a mode time that is a factor of two smaller than $T(O_X)$. Since at least the 1970s, atmospheric chemistry modelling has recognized that stratospheric O_3 responded to perturbations more slowly than the photolysis time scale, and researchers effectively intuited the eigenvalue decomposition by defining O_X with its time-scale. The decomposition, however, includes the effect of quadratic loss of O_X and has the correct time scale, $[O_X]/4R_4$.

4. Tropospheric methane chemistry: delayed recovery of a perturbation

The conundrum presented by Don Fisher in 1993 at a workshop on stratospheric ODP led to the discovery that chemical coupling of methane (CH_4), carbon monoxide (CO) and hydroxyl radicals (OH) would extend the effective lifetime of atmospheric CH_4 perturbations. Using a two-dimensional global chemistry–transport model (CTM), Fisher (1995) reported that a pulse of CH_4 added to the atmosphere did not decay with the expected e-fold time equal to the CH_4 steady-state lifetime (e.g. 8 yr), but with one that was notably longer (e.g. 12 yr). Moreover, the time scale of this delayed recovery was constant, independent of the magnitude of the perturbation, indicating that a nonlinear chemical response was not the cause. Earlier, Isaksen & Hov (1987) had noted the importance of the CH_4–OH feedback in a global model, when a small increase (e.g. 10%) in global CH_4 emissions produced a larger relative increase (e.g. 14%) in steady-state CH_4 abundance. These phenomena were generally regarded as the result of a nonlinear response that would disappear for small perturbations. The formal relationship between the steady-state feedback and Fisher's time scales was not immediately recognized.

In response to Fisher's problem, Prather (1994, 1996) developed a simple one-box chemistry model that demonstrated how chemical feedbacks could alter the time scale of CH_4 perturbations. Manning (1999) updated this model and applied it to carbon isotopes, but in this example, the original box model is retained. Consider a simplified model of the CH_4–CO–OH chemical system as having three reactions

(i) $CH_4 + OH \Rightarrow \cdots \Rightarrow CO$ $R_5 = k_5[CH_4][OH]$ $k_5 = 1.266 \times 10^{-7} \, \mathrm{s}^{-1} \, \mathrm{ppt}^{-1}$

(ii) $CO + OH \Rightarrow \cdots$ $R_6 = k_6[CO][OH]$ $k_6 = 5.08 \times 10^{-6} \, \mathrm{s}^{-1} \, \mathrm{ppt}^{-1}$

(iii) $OH + X \Rightarrow \cdots$ $R_7 = k_7[X][OH]$ $k_7[X] = 1.062 \, \mathrm{s}^{-1}$,

and three constant source terms (parts per trillion (ppt)=picomoles per mole; parts per billion (ppb)=nanomoles per mole):

$$S_{CH_4} = 177 \, \mathrm{ppb} \, \mathrm{yr}^{-1} \quad S_{CO} = 240 \, \mathrm{ppb} \, \mathrm{yr}^{-1} \quad S_{OH} = 1464 \, \mathrm{ppb} \, \mathrm{yr}^{-1}.$$

Reaction (5) has intermediate steps (not shown) that produce CO. The X in reaction (7) is a class of species that are an important sink for OH. The continuity equations are

$$\frac{\mathrm{d}[CH_4]}{\mathrm{d}t} = S_{CH_4} - R_5$$

$$\frac{\mathrm{d}[CO]}{\mathrm{d}t} = S_{CO} + R_5 - R_6$$

$$\frac{\mathrm{d}[OH]}{\mathrm{d}t} = S_{OH} - R_5 - R_6 - R_7.$$

The rate coefficients and source terms are chosen to represent average tropospheric conditions and give steady-state abundances typical of the current atmosphere:

$$[CH_4] = 1704 \, \mathrm{ppb} \quad [CO] = 100 \, \mathrm{ppb} \quad [OH] = 0.026 \, \mathrm{ppt}.$$

The Jacobian (J) of the chemical system is calculated from

$$J = \begin{pmatrix} \dfrac{\partial\left(\dfrac{\mathrm{d}[CH_4]}{\mathrm{d}t}\right)}{\partial[CH_4]} & \dfrac{\partial\left(\dfrac{\mathrm{d}[CH_4]}{\mathrm{d}t}\right)}{\partial[CO]} & \dfrac{\partial\left(\dfrac{\mathrm{d}[CH_4]}{\mathrm{d}t}\right)}{\partial[OH]} \\[3em] \dfrac{\partial\left(\dfrac{\mathrm{d}[CO]}{\mathrm{d}t}\right)}{\partial[CH_4]} & \dfrac{\partial\left(\dfrac{\mathrm{d}[CO]}{\mathrm{d}t}\right)}{\partial[CO]} & \dfrac{\partial\left(\dfrac{\mathrm{d}[CO]}{\mathrm{d}t}\right)}{\partial[OH]} \\[3em] \dfrac{\partial\left(\dfrac{\mathrm{d}[OH]}{\mathrm{d}t}\right)}{\partial[CH_4]} & \dfrac{\partial\left(\dfrac{\mathrm{d}[OH]}{\mathrm{d}t}\right)}{\partial[CO]} & \dfrac{\partial\left(\dfrac{\mathrm{d}[OH]}{\mathrm{d}t}\right)}{\partial[OH]} \end{pmatrix}$$
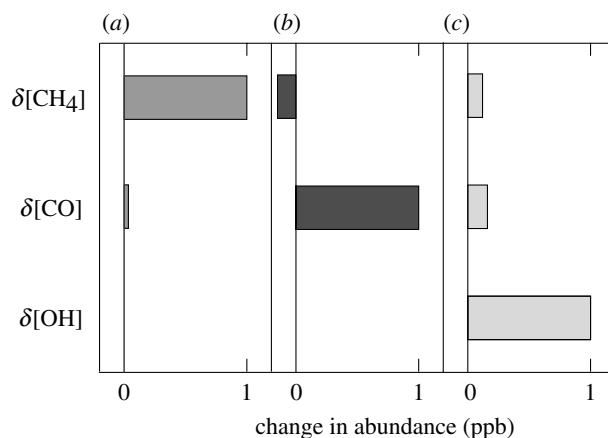
Figure 1. Three eigenvectors of the CH_4–CO–OH system (see text) are labelled with their mode times. For each vector, the bars indicate the perturbation in absolute abundance (e.g. ppb). Each mode is scaled to have the maximum perturbation as $+1$ ppb. The amplitude of the OH perturbation for the first two modes is less than 10^{-7} and does not show. (*a*) No. 1, 13.6 years, (*b*) no. 2, 0.285 years and (*c*) no. 3, 0.56 s.

and at steady state has the value (all units are yr^{-1})

$$J = \begin{array}{ccc} -0.104 & 0 & -6.81 \times 10^6 \\ +0.104 & -4.17 & -9.23 \times 10^6 \\ -0.104 & -4.17 & -56.4 \times 10^6. \end{array}$$

The diagonal elements are the negative inverse of the traditionally defined lifetimes

$$9.6 \text{ yr}(CH_4) \quad 0.240 \text{ yr}(CO) \quad 0.56 \text{ s}(OH).$$

The three inverse negative eigenvalues (mode times) of J differ from these lifetimes owing to the chemical coupling (i.e. the off-diagonal terms)

$$13.6 \text{ yr} \quad 0.285 \text{ yr} \quad 0.56 \text{ yr}.$$

The corresponding eigenvectors are shown in figure 1. Given the relative species abundances in each mode and the mode time of each, one can easily identify the first as the CH_4-like chemical mode but with a time scale 40% longer than the CH_4 lifetime, the second as the CO-like chemical mode with a 20% longer time scale and the third as the OH-dominated mode with a time scale equal to the OH lifetime. In this case, chemical coupling (i.e. off-diagonal terms in J) has shifted the smallest two eigenvalues, but left the time scale of the most rapid process unchanged.

A 1 ppb perturbation to CH_4 alone can be decomposed into modes using the inverse of the eigenvector matrix. It is composed of 0.995 ppb in the first mode, 0.005 ppb in the second and less than 0.001 ppb in the extremely short-lived third mode. The analytical solution is then

$$\delta[CH_4](t) \approx +0.995 \, e^{-t/13.6} + 0.005 \, e^{-t/0.285} \text{ ppb},$$
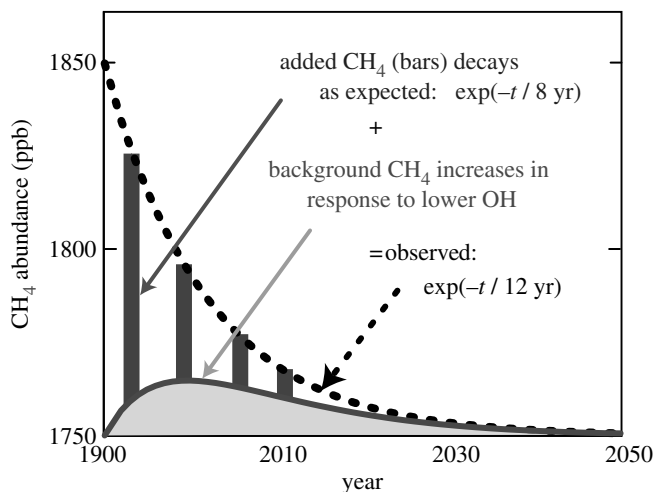
Figure 2. Simulated atmospheric decay of a CH_4 perturbation of 100 ppb. If tagged, the added CH_4 (bars) would be seen to decay with an e-fold nearly equal to the CH_4 steady-state lifetime of 8 yr. The increase in background CH_4 (baseline) caused by the lower OH induced by the perturbation, however, yields a net overall decay time for all CH_4 molecules (dashed line) of 12 yr.

and thus most of the perturbation decays with the 13.6-yr mode time. Since the long-lived mode also has CO and OH components, the other species also have decadal perturbations:

$$\delta[CO](t) \approx +0.035\, e^{-t/13.6} + 0.035\, e^{-t/0.285} \text{ ppb}$$

$$\delta[OH](t) \approx -4.5 \times 10^{-6}\, e^{-t/13.6} \text{ ppt.}$$

Likewise, a 1 ppb perturbation to CO alone excites all the three modes. The 0.15 ppb perturbation to CH_4 caused by the chemical coupling is initially masked but appears as the bulk of the CO perturbation decays in a few months. It decays with the characteristic 13.6-yr mode time:

$$\delta[CO](t) \approx +0.005\, e^{-t/13.6} + 0.995\, e^{-t/0.285}$$

$$\delta[CH_4](t) \approx +0.15\, e^{-t/13.6} - 0.15\, e^{-t/0.285}.$$

Can this help us understand Fisher's results? The amount of CH_4 added to the model atmosphere was small enough that OH did not change by more than a few per cent. Thus, if the added CH_4 could be tagged, we would see it decay with the expected lifetime of 8 yr. However, the background CH_4 increased in response to the lowered OH, and thus the apparent decay rate for total CH_4 is the mode time of 12 yr (figure 2). The Isaksen and Hov results can be understood if one accepts that while the steady-state lifetime for the *global* CH_4 burden is about 8 yr, that for *additional* emissions is 12 yr (see also §7). The simple model above, when confirmed by the three-dimensional atmospheric chemistry models, resulted in a $+40\%$ revision to the IPCC's GWP for CH_4 (Prather *et al.* 1995; Ramaswamy *et al.* 2001).

5. Time scales for methyl bromide: transport between reservoirs

Methyl bromide (CH_3Br), an ozone-depleting substance (ODS), is emitted into the atmosphere through natural, primarily oceanic, processes. Over the past few decades, humans have increased its atmospheric abundance through synthetic production and use as a fumigant for agricultural fields, structures and harvested crops. In the atmosphere, CH_3Br is lost with time scales of order a year through reaction with OH and by photolysis in the stratosphere. It delivers inorganic bromine $(Br_Y = Br + BrO + HOBr + HBr + BrONO_2 + BrCl + \cdots)$ to the stratosphere, where Br-catalysed reactions destroy O_3. There has been confusion (e.g. Butler 1994) over the definition of lifetime for a gas like CH_3Br with multiple reservoirs and further misunderstanding over the time scales of atmospheric response that affect its categorization as an ODS.

A simplified, yet realistic, model for CH_3Br and Br_Y has been analysed in terms of chemical modes and time scales (Prather 1997). Take a one-dimensional profile through the troposphere ($z = 0–14$ km) and the stratosphere ($z = 14–52$ km) with pressure $p(z) = 10^{-z/16}$ atm and molecular density $N(z) = 2.4 \times 10^{19} p(z)$ cm^{-3}. Transport is through vertical diffusion with rapid mixing in the troposphere ($K(z) = 3 \times 10^5$ cm^2 s^{-1} for 0–12 km) and a typical stratospheric diffusion profile ($K(z) = 3 \times 10^3 p(14)/p(z)$ cm^2 s^{-1} for 14–52 km). Photochemical loss of CH_3Br is assumed to occur at a constant frequency of 2.17×10^{-8} s^{-1} from 0 to 10 km and as $6 \times 10^{-12} p(z)^{-2}$ s^{-1} above 10 km. For Br_Y, assume that all CH_3Br loss equals Br_Y production and that the only loss of Br_Y is through rainout in the troposphere with a frequency of 2.315×10^{-6} s^{-1}. These parameters are representative of the average values in the multidimensional atmospheric chemistry models.

With surface emissions of 90×10^6 kg yr^{-1} of CH_3Br, a steady-state profile builds up with 10 ppt at the surface level as shown in figure 3 (solid line). The atmospheric burden is approximately 157×10^6 kg, and thus the steady-state lifetime is 1.75 yr. If all emissions cease, then the decay of CH_3Br from the atmosphere develops a prominent nose, with an e-fold time of 2.10 yr (dashed lines in figure 2). Where do this pattern and time scale come from?

In this case, the chemistry is linear and fixed and, ignoring Br_Y for now, there is only one species. Thus, the coupled chemical modes arise only through the transport operator in the continuity equation. The continuum in z has been discretized by solving for CH_3Br at 14 grid points: $z_i = 0, 4, 8, 12, 16, 20, \ldots, 48, 52$ km. A set of 14 continuity equations are entirely linear, using second-order finite-difference (diffusion) equations at interior points to couple the nearest neighbours and second-order flux boundary conditions at $z = 0$ and 52 km. With appropriately normalized flux boundary conditions, the Jacobian derived from the continuity equation at each level z_i is a 14×14 tridiagonal matrix with units of inverse time. If Br_Y is included, then the Jacobian is 28×28 and block tridiagonal with 2×2 blocks. In either case, it is easily solved for all eigenvalues and eigenvectors. Since there is no chemical feedback of Br_Y on CH_3Br in this system, the 14 eigenvalues/vectors of the 14×14 CH_3Br system are unchanged in the 28×28 matrix.

The 14 eigenvectors for the CH_3Br system are shown in figure 4 and labelled with their time constants. Most of the modes are short-lived, contain alternate signs (zero net mass) and represent mass-conserving diffusive exchange between the neighbouring points. The second longest-lived mode (1.34 yr) appears to be
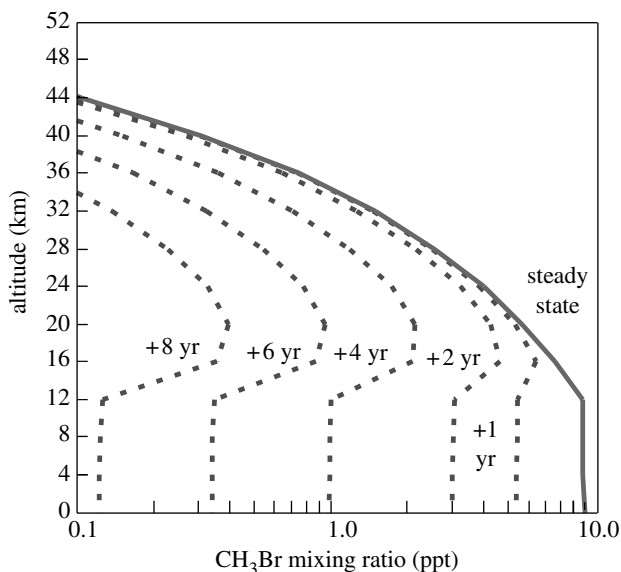
Figure 3. Profile (solid line) of CH_3Br mixing ratio (ppt) versus altitude (km) at steady state driven by surface emissions. Also shown are the successive profiles (dashed lines) for years 1, 2, 4, 6 and 8 following cut-off of CH_3Br emissions. Initial loss of CH_3Br occurs at a rate $(1.75 \text{ yr})^{-1}$ given by the steady-state lifetime, but slows in a few years to that of the longest-lived mode time $(2.10 \text{ yr})^{-1}$ with the pattern of that mode (figure 4).

an exchange between the troposphere and the stratosphere. The longest-lived mode (2.10 yr) matches the pattern and time scale of the long-term decay seen in figure 3. The 10 ppt CH_3Br in the $z = 0$ level consists of 4.8 ppt e-folding at 2.10 yr, 5.0 ppt at 1.34 yr, 0.1 ppt at 0.02 yr and a small amount of the other 11 modes. Thus, the decomposition into modes allows analytical prediction of long-term behaviour equivalent to the numerical integration of the continuity equation and, further, helps identify the time scales and patterns of transport between reservoirs.

6. Time scales for nitrous oxide: radiative coupling through ozone

Nitrous oxide (N_2O), a greenhouse gas, is also a dominant source of stratospheric nitrogen oxides ($NO_Y = NO + NO_2 + HNO_3 + N_2O_5 + \cdots$), which catalytically destroy O_3. The currently observed increase in N_2O is consistent with an increasing emission source from the agricultural use of nitrogen, poses a threat to the ozone layer and contributes to global warming. Analysis of a linearized one-dimensional troposphere–stratosphere model of the N_2O–NO_Y–O_3 system in terms of chemical modes (Prather 1998) shows how the radiative coupling through O_3 shortens the time for atmospheric decay of N_2O perturbations.

In the stratosphere, N_2O is destroyed by direct photolysis and reaction with meta-stable $O(^1D)$. Both reactions are controlled by O_3: locally, photolysis of O_3 is the source of $O(^1D)$; and globally, O_3 absorbs ultraviolet sunlight, thus limiting the photolysis rates. Stratospheric NO_Y is produced by the reaction of $O(^1D)$
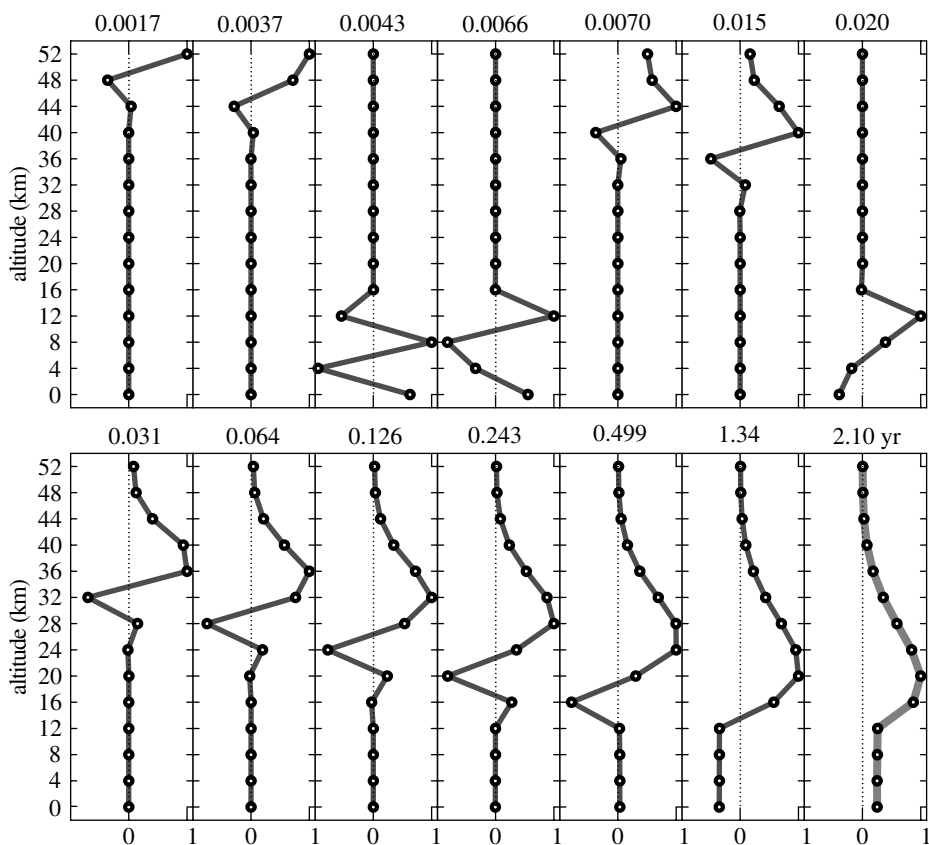
Figure 4. Complete set of 14 chemical modes (eigenvectors) for the one-dimensional CH_3Br diffusion model (see text) in the order of increasing mode time (yr) shown above each. Eigenvectors are normalized to an absolute maximum of $+1$.

with N_2O and destroyed by washout in the troposphere and photolytic loss above 40 km. NO_Y enhances photochemical destruction of O_3. Thus, even locally, the N_2O–NO_Y–O_3 system is a fully coupled chemical system, like the CH_4–CO–OH system. A simple model includes vertical diffusion between the stratosphere and the troposphere as for CH_3Br above, assumes rapid removal of NO_Y and O_3 below 10 km and linearizes stratospheric photochemistry in terms of the three variables (N_2O, NO_Y and O_3) about typical atmospheric conditions. The continuity equations can be solved for the steady state forced by an emission source of N_2O in the surface level (figure 5a). The Jacobian becomes a 42×42 block tridiagonal matrix with 3×3 blocks at each of the 14 vertical levels (for details, see Prather 1998). Chemical coupling is local and occurs through the 3×3 blocks along the diagonal. Transport coupling is between the neighbouring levels and is represented by the off-diagonal blocks. Since the abundance of O_3 in any layer affects the absorption and scattering of ultraviolet sunlight, and hence the photolysis rates in all layers, the radiative coupling is across all levels. Thus, the Jacobian is a sparse, but full matrix, which can nevertheless be readily solved for the chemical modes.
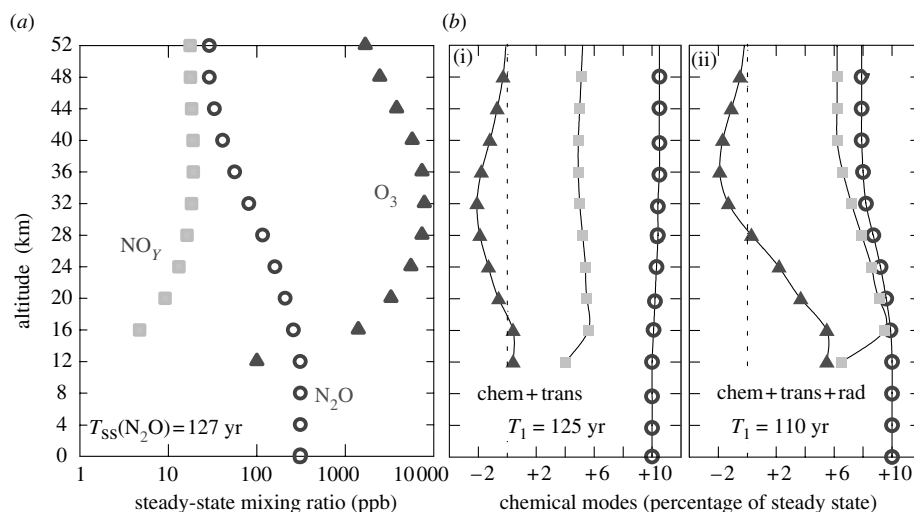
Figure 5. (*a*) Steady-state altitude profiles (parts per billion) of N_2O (open circles), NO_Y (squares) and O_3 (triangles) calculated from the one-dimensional photochemical model described in the text. Tropospheric abundances of NO_Y and O_3 are very small and not shown. The steady-state lifetime for N_2O forced by emissions into the lowest level is 127 yr. (*b*) Altitude profiles of the longest-lived chemical mode of the N_2O–NO_y–O_3 system, (i) when only local chemistry and diffusive transport are included (e-fold time $T_1 = 125$ yr) and (ii) when radiative coupling through O_3 is also included ($T_1 = 110$ yr). The two modes are scaled to $+10\%$ of the steady-state abundance of N_2O in the surface level, and the profiles are plotted as percentage change relative to the steady-state profiles shown in (i).

Without the radiative coupling, the longest-lived mode has a mode time (T_1) of 125 yr, close to the steady-state lifetime from the surface-level emissions, $T_{SS} = 127$ yr. The pattern of this mode (figure 5*b*(i)) shows uniform perturbations in N_2O and similar perturbations in NO_Y with half the relative amplitude. In O_3, the model produces a smaller relative depletion (opposite sign) centred about 32 km, where NO_Y-catalysed ozone destruction has its largest impact. The similarity of these two time scales almost justifies the use of T_{SS} as the e-folding time for N_2O emissions that is used in GWP and ODP calculations (e.g. Solomon *et al.* 1992). With radiative coupling (figure 5*b*(ii)), however, T_1 drops to 110 yr, the profile of the N_2O perturbation changes slightly, the NO_Y perturbation almost doubles and the O_3 self-healing effect gives positive perturbations in the lower stratosphere. Unlike the tropospheric CH_4–CO–OH system, the N_2O–NO_Y–O_3 system has negative feedbacks: increasing N_2O reduces O_3 in the middle stratosphere, allowing solar ultraviolet to destroy N_2O more rapidly.

Having solved for all 42 eigenvectors, we can readily analyse perturbations. Three patterns of N_2O perturbation are decomposed into the chemical modes with the six longest time scales shown in table 1. A perturbation of 1000 kg matching the surface-forced steady-state profile is almost entirely mapped onto mode 1 (110-yr e-fold), but 1000 kg put entirely into the surface level (effectively 0–1 km) has 1025 kg in mode 1 with the balance made up of both positive and negative amounts in the short-lived modes. As expected, placing 1000 kg at 40 km has a much smaller impact on the long-term burden of N_2O with only 22 kg in mode 1,

Table 1. Decomposition of a perturbation into kilogram (N_2O) in the first six modes of the N_2O–NO_Y–O_3 system.

perturbation	mode (yr)					
	110	3.1	2.0	0.68	0.66	0.60
1000 kg N_2O at SS[a]	999.5	0	1	0	0	1
1000 kg N_2O at 0 km	1025	2	-34	-2	1	9
1000 kg N_2O at 40 km	22	-17	156	-74	28	252
-10 DU of O_3 >28 km	-20	0	-10	3	-5	-8

[a]Steady state as forced by continuous emissions at 0 km.

and most of the 1000 kg going into short-lived modes (not shown), giving a steady-state lifetime for N_2O of about 3 yr! A large ozone perturbation of -10 Dobson units (approx. 3% of the total column), such as might result from a very large solar proton event, mostly recovers within weeks, but leaves behind a century-long deficit of 20 kg N_2O in mode 1 (as summarized in table 1).

After this analysis, several multidimensional full chemistry models (Prather *et al.* 2001) examined the decay of an N_2O perturbation and confirmed that the perturbation e-fold time was on average 8% less than the surface-emission steady-state lifetime.

7. Integrating over environmental impacts: the magic of steady state

The steady-state pattern of trace species for specified emissions can be readily calculated using the chemical modes. Following the notation of §2, consider a perturbation, $\delta V_{SS}(x, y, z, n)$, that is the steady-state response to regular periodic emissions of trace species (n). One can treat emission sources as the addition of trace species (n) to specific (x, y, z) locations or equivalently as a source pattern $S(x, y, z, n)$, which can be decomposed into the dimensionless eigenvectors (modes) E_i with coefficients b_i, $S = \sum_{i=1:m} b_i E_i$. An infinitesimal amount of emissions, $S\,\mathrm{d}t$ (kg), from time t in the past would have decayed according to each mode time, $\sum_{i=1:m} b_i E_i \exp(-t/T_i)\mathrm{d}t$. The steady-state perturbation is, by definition, the integral of $S\,\mathrm{d}t$ from minus infinity to the present,

$$\delta V_{SS} \equiv \int_{-\infty}^{0} S\mathrm{d}t = \sum_{i=1:m} b_i E_i \left(\int_{-\infty}^{0} \exp(-t/T_i)\mathrm{d}t \right) = \sum_{i=1:m} T_i b_i E_i.$$

Assume that the source pattern S comprises only emissions of species (n), but allow for the perturbation δV_{SS} to include all species (n'). The mass operator M^n, defined in §2, computes the global emissions rate (kg yr^{-1}) of species (n) in the source pattern, $M^n[S] = \sum_{i=1:m} b_i m_i^n$(kg yr^{-1}), and also the global burden (kg) in the steady-state perturbation, $M^n[\delta V_{SS}] = \sum_{i=1:m} T_i b_i m_i^n$(kg), where $m_i^n = M^n[E_i]$ is dimensionless. Thus, the steady-state lifetime of species (n) depends on the source pattern S through the coefficients b_i:

$$T_{SS}(n) \equiv \frac{M^n[\delta V_{SS}]}{M^n[S]} = \frac{\sum_{i=1:m} T_i b_i m_i^n}{\sum_{i=1:m} b_i m_i^n} \text{(yr)}.$$

A critical quantity in evaluating the overall environmental impact of a trace gas, such as the ODP or global warming potential, is the integrated abundance of the gas following a brief emission pulse. This integral needs to include not only the decay of the primary source gas, but also the accumulation and decay of any secondary products that impact radiative forcing or ODP. Thus, the general form will be the integrated change in species (n') at some location (x', y', z') following the initial perturbation represented by an emission pattern $S(x, y, z, n)$ over a brief period Δ. For a short pulse of emissions, $S\Delta$ (kg), the atmospheric perturbation $\delta[V_\Delta(t)] = \sum_{i=1:m} \Delta b_i E_i \exp(-t/T_i)$ can be integrated forward in time to give the integrated impact, II (kg-yr),

$$II(S\Delta) = \int_{t=0:\infty} \delta V_\Delta(t)\mathrm{d}t = \Delta \sum_{i=1:m} T_i b_i E_i(x, y, z, n') = \Delta \delta V_{SS}(x, y, z, n').$$

It can be rewritten using the definition of $T_{SS}(n)$ as

$$II(S\Delta) = \delta V_{SS}(x, y, z, n') T_{SS}(n) \left(\frac{M^n[S\Delta]}{M^n[\delta V_{SS}]} \right).$$

Thus, the overall integrated perturbation caused by emission of a trace gas, including all secondary impacts, is given exactly by the steady-state pattern in all species multiplied by the steady-state lifetime of species (n) and then scaled by the ratio of the amount of n in the pulse to that in the steady-state pattern.

As an example, consider the ODP in response to the release of CH_3Br at the surface. The ozone depletion can be approximated by the perturbation to Br_Y at 20 km as shown in figure 6. There is a delay in the impact, as CH_3Br is transported into the stratosphere and is chemically converted into Br_Y (dark grey solid line). A peak in Br_Y is reached *ca* 6 yr following the release and is followed by a slow decay with the mode time of 4.52 yr, corresponding to the removal of a conservative tracer from the stratosphere. In this case, the release (kg) is scaled to be the amount of CH_3Br present in the atmosphere for a steady-state distribution forced by surface emissions resulting in 1 ppt at the surface. The area under the Br_Y curve is 0.73 ppt-yr. As shown above, this integral is exactly equal to the product of the steady-state lifetime for CH_3Br with surface emissions (1.75 yr) and the steady-state abundance of Br_Y at 20 km (0.42 ppt). It is almost universally assumed in assessments of ODP or climate forcing (Solomon *et al.* 1992; WMO 1995; IPCC 1996) that this integral is represented by a single e-fold decay of 1.75 yr (light grey solid line). Fortunately, the integrated impact is correctly evaluated with this assumption, but the time scale is not. Even with a 2.5-yr delay to allow for CH_3Br to reach the stratosphere (dashed line), the time scale of the response is incorrect (see Ko *et al.* 1997 for discussion). This mistaken view of time scales has led to the false reasoning in Montreal Protocol negotiations that reductions in CH_3Br would provide recovery of ozone within a few years: they do not.

The theory developed here applies readily to very short lived species, such as 1-C_3H_7Br, with a tropospheric residence time of weeks (Bridgeman *et al.* 2000; Olsen *et al.* 2000, Wuebbles *et al.* 2001). It provides a formal basis for computing the environmental impact using the readily calculated annual steady-state pattern of impacts (e.g. Br_Y) scaled by the annual steady-state lifetime of the source gas.
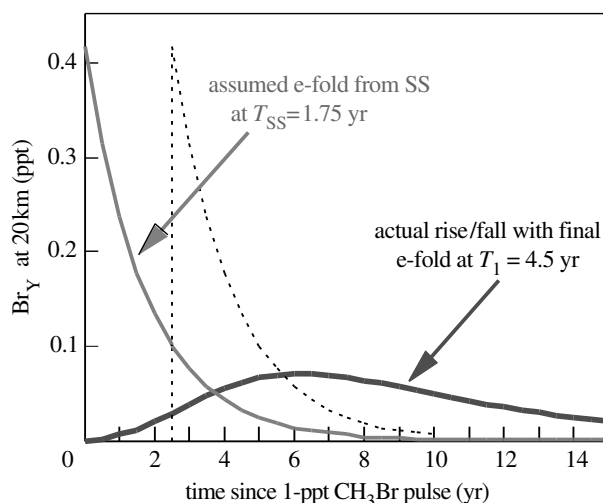
Figure 6. Temporal behaviour of Br_Y (ppt) at 20 km in response to a single release of CH_3Br in the lowest level (0–1 km). The total release of CH_3Br (kg) is equivalent to the amount in a steady-state pattern from surface emissions ($T_{SS} = 1.75$ yr) that maintain 1 ppt at the surface and also 0.417 ppt of Br_Y at 20 km. It is usually assumed that the Br_Y response to the CH_3Br release is represented by the steady-state level of Br_Y decaying with the e-fold time of T_{SS} (dark grey solid line): $Br_Y(t) = 0.417\ e^{-t/1.75}$. Sometimes a lag of 2.5 yr is adopted to approximate the delay in transport from troposphere to stratosphere (thin dashed line). The integrated area under this curve represents the cumulative environmental impact (e.g. on ozone depletion) of 0.73 ppt-yr. Neither case resembles the true rise and fall of Br_Y at 20 km following the release of CH_3Br (dark grey solid line): $Br_Y(t) = 0.588\ e^{-t/4.52} - 1.847\ e^{-t/2.10} + 1.853\ e^{-t/1.34} - 0.594\ e^{-t/0.892} - 0.147\ e^{-t/0.499} + 0.191\ e^{-t/0.387} - 0.084\ e^{-t/0.243} + 0.040\ e^{-t/0.207}$. This curve can be simply integrated from the individual exponential terms (although some give a seemingly non-sensical negative impact) to give 0.73 ppt-yr, the same integral value as the steady-state e-fold but with a delayed impact.

8. Distinct modes: the infinite continuum

A concern with the simplified stratosphere–troposphere model used here is that the results are specific to the discrete finite grid used to solve the continuous diffusion equation. To test this, we experiment with the one-dimensional diffusion model, assuming zero flux at the top and a rapid loss ($0.01\ s^{-1}$) only in the surface layer. Such a model should describe the stratospheric decay of a perturbation to a conserved species like Br_Y, Cl_Y or SF_6. (Note that decay is more rapid for a species like NO_Y with loss in the upper stratosphere.) The existence of distinct chemistry–transport modes is found even for the limiting case of a continuous semi-infinite atmosphere.

With the top at 52 km, increasing the vertical resolution from 4 to 1/4 km increases the number of eigenvalues in the one-dimensional troposphere–stratosphere model from 14 to 224. The evolutions of the four longest mode times (the smallest absolute eigenvalues) are shown in figure 7. Although all four mode times decrease by approximately 25% as the resolution increases, they remain separated and unique. Convergence of the values is apparent, and the difference between mode times on a grid size of 1 km and those in the continuous limit is approximately 10%.
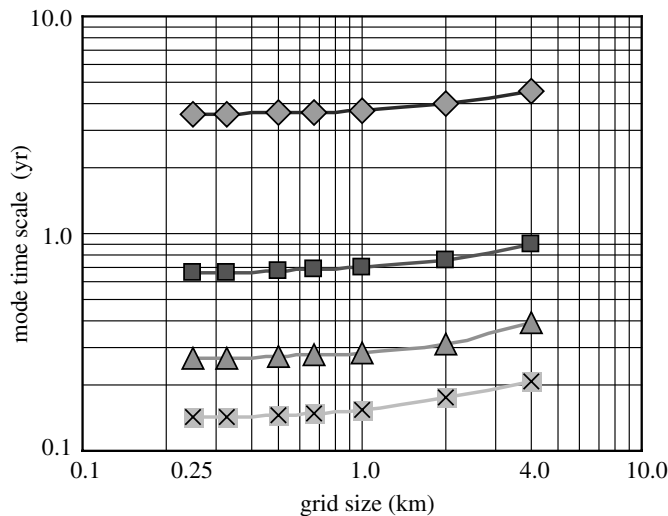
Figure 7. Convergence of the four longest mode times in a one-dimensional diffusion model as the grid size decreases from 4 to 0.25 km. The model has typical troposphere–stratosphere diffusion coefficients (see text) with zero flux at the top ($z=52$ km) and rapid loss ($0.01\,\mathrm{s}^{-1}$) only in the surface layer ($z=0$ km).

Providing a solution for the modes on a semi-infinite atmosphere poses a different problem. With an infinite upper boundary and constant diffusion coefficient K, Waugh & Hall (2002, reaction 9) show that the Green's function used for age of air has an analytical form that precludes the simple exponential decay of the eigenvalue decomposition. In the stratosphere, typical profiles for K have it increasing as density N decreases (Ehhalt *et al.* 2004), and thus far we have chosen $K \to N^{-1}$. In this test, three cases are chosen near the Waugh and Hall limiting form: (i) $K \to N^{-0.05}$, (ii) $K \to N^{-0.01}$, and (iii) $K \to$ constant. Leaving the grid step at 4 km, the one-dimensional model top is increased from 68 to 828 km (18 to 208 modes), and the evolution of the four longest mode times for each case is shown in figure 8. For case (i), the four solid lines show increasing mode times until the top reaches 200 km, with no change thereafter. For more slowly increasing K, case (ii), the four dashed lines show similar behaviour although the second through fourth longest mode times are still shifting even when the top reaches 828 km. For the previous examples with $K \to N^{-1}$, the four longest mode times have converged to within 1% when the model top reaches 68 km. For case (iii), however, raising the upper boundary indeed changes the character of the chemistry–transport modes (dotted lines), and we approach a continuum of long-lived modes as anticipated.

9. The stratospheric decay mode: observed age of air, tritium and chlorine

The age of air in the stratosphere is defined as the time since the air was last in the troposphere, and the mean age can be directly observed with quasi-conserved trace gases that are increasing at a regular rate (e.g. CO_2, SF_6). In models, the
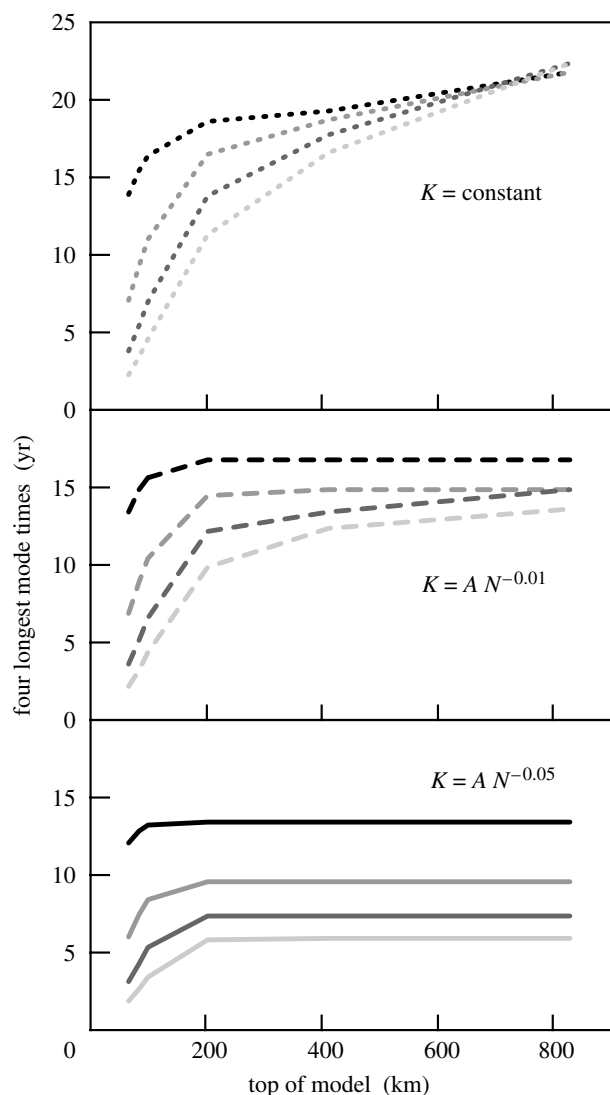
Figure 8. Convergence of the four longest mode times in a one-dimensional diffusion model (figure 7) as the top of the model increases from 68 to 828 km. Results are shown for different dependences of the diffusion coefficients K on the density N: $K = \text{constant } A$ (four dotted lines), $K = AN^{-0.01}$ (dashed lines) and $K = AN^{-0.05}$ (solid lines). An infinite atmosphere with constant K has no modes (dotted), but if K has only a slight inverse dependence on N, then the long-lived modes appear as distinct even as the upper boundary approaches infinity.

age of air can be calculated as a spectrum of ages from which the mean age can be evaluated (Waugh & Hall 2002). The mean age is related to the chemical modes. Specifically, the tail end of the spectrum corresponds to the mode describing stratospheric decay of a conserved tracer (see discussion above and Hall *et al.* 1999). The observed decay of stratospheric tritium (^{3}H) injected by atmospheric nuclear tests in the 1960s looks like a chemical mode (Ehhalt *et al.* 2004). The lag in recovery of upper stratospheric HCl following the decline of tropospheric

chlorofluorocarbons and other halocarbons in the 1990s is also a measure of the age of air spectrum and the long-lived modes (see discussion in Waugh & Hall 2002). Together, these observations provide the only current observational test of chemical modes.

A clear demonstration of the stratospheric decay mode was found with the Models and Measurements II project (Hall *et al.* 1999). For each model used to compute the age-of-air spectra, the original request had been to integrate 10–20 yr to ensure that the tail of the spectrum was well defined. Recognition that this tail represented the decay mode and that for each model it followed the same exact e-fold time throughout the stratosphere, however, enabled substantial savings in computation and a far easier evaluation of the mean age only after 6–10 yr of integration. In addition, Hall *et al.* (1999) and Ehhalt *et al.* (2004) showed that for all but one of the three-dimensional models, there was a simple linear relationship between the mean age at 30 km and the decay mode's e-fold time.

Several years after injection, the decay of stratospheric tritium (as water above 20 km) followed a single exponential decay from 1969 to 1984. When corrected for the radioactive decay of tritium, this gives a decay mode time of 7.7 ± 2 yr (Ehhalt *et al.* 2004). Allowing for a trend in stratospheric water that is consistent with the limited measurements, this decay mode time drops to 6.9 years. Corresponding mode times derived from the observed mean age range from 3.8 to 5.3 yr. Given the uncertainties associated with both of these derivations, a mode time between 5 and 6 yr is probable. Unfortunately, these values are still outside the range of decay mode times for all but one of the three-dimensional models, i.e. 1.44–4.75 yr (see table 2 of Ehhalt *et al.* 2004).

10. Chemistry–transport modes: three-dimensional tropospheric chemistry

In realistic simulations of global atmospheric chemistry with a three-dimensional chemistry–transport model (CTM), the continuity equation operators (Chem, Trans and Rad) change every hour or so. Presuming that this change is cyclic (e.g. the 24 h cycle of photolysis rates, the seasonal cycles of meteorological transport), the chemical modes should still exist but include another dimension that describes the temporal behaviour of perturbations over the daily/yearly cycle; e.g. $E_i(x, y, z, n, t)$. Indeed, the existence of the long-lived, seasonally varying, CH_4-like, tropospheric chemistry mode has been sought for and characterized in at least two CTMs (Wild & Prather 2000; Derwent *et al.* 2001). The stratospheric decay mode was identified after the fact in many CTMs through the age-of-air experiments (Hall *et al.* 1999).

The number of CTM modes with an annually repeating meteorology readily exceeds 10^8, precluding the complete chemical mode decomposition shown in §§3–8. The longest-lived mode, however, can still be characterized by following the decay of perturbations. Wild & Prather (2000) and Derwent *et al.* (2001) found the decadal tropospheric mode (CH_4–CO–OH–NO_x–$\cdots$) of their CTMs by tracking a perturbation run minus control run for a decade following several different perturbations to tropospheric chemistry. (These CTMs did not include feedbacks with stratospheric chemistry that would have excited the century-long stratospheric N_2O-like mode.)
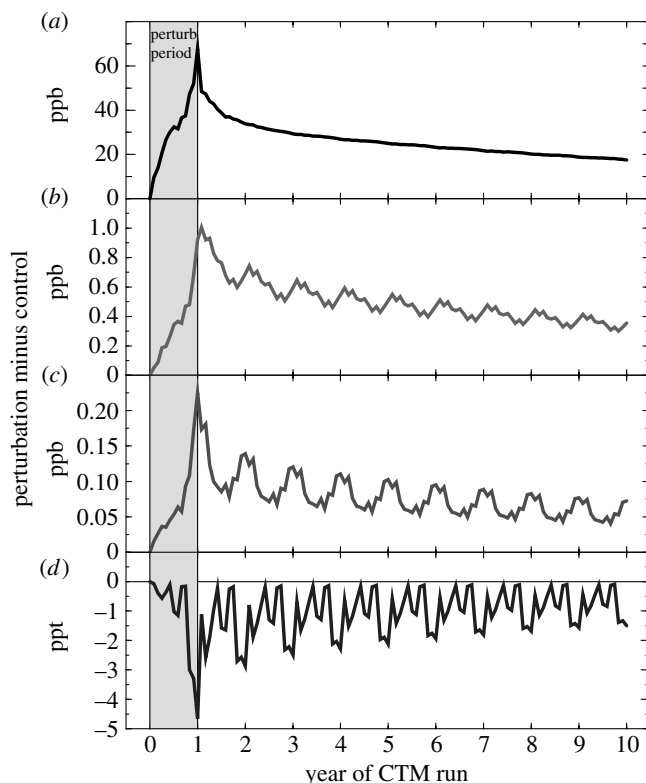
Figure 9. Perturbations to (*a*) CH$_4$ (ppb), (*b*) CO (ppb), (*c*) O$_3$ (ppb) and (*d*) NO$_x$ (ppt) at Mace Head, Ireland (53° N, 10° W) caused by a 1-yr, 20% increase in global CH$_4$ emissions. The decay of this perturbation is followed for 9 yr after return of CH$_4$ emissions to normal levels. Results are shown for the perturbation minus control runs with a three-dimensional global chemistry–transport model.

In one numerical experiment, Wild *et al.* increased global CH$_4$ emissions by 20%. The resulting perturbations to the CH$_4$, CO, O$_3$ and NO$_x$ abundances simulated for Mace Head, Ireland are shown in figure 9. During the perturbation year, abundances of CH$_4$, CO and O$_3$ rise, while that of NO$_x$ falls. After the perturbation to emissions ceases (year 1), there are rapid decays involving short-lived modes, but within a few years, the perturbation curves assume the regular pattern of a repeating annual cycle that decays over any 12-month period with an e-fold time of 14.2 yr. Wild *et al.* extracted the longest-lived mode from these experiments, and the zonal-mean, mid-tropospheric, latitude-by-season patterns of CH$_4$ and CO are shown in figure 10. The modes are dimensionless and are scaled to an absolute abundance of a single species as one point in space and time. In this example, the mode has been scaled to have an annual mean CH$_4$ perturbation of 100 ppb. The e-fold has been removed to show the annually repeating patterns. The seasonal variation in the CH$_4$ perturbation, 98–102 ppb, is similar to that in CO, 1–3 ppb, but with opposite phase in both latitude and season. The large annual variations of the mode at mid-latitudes indicate the importance of seasonal photochemistry.
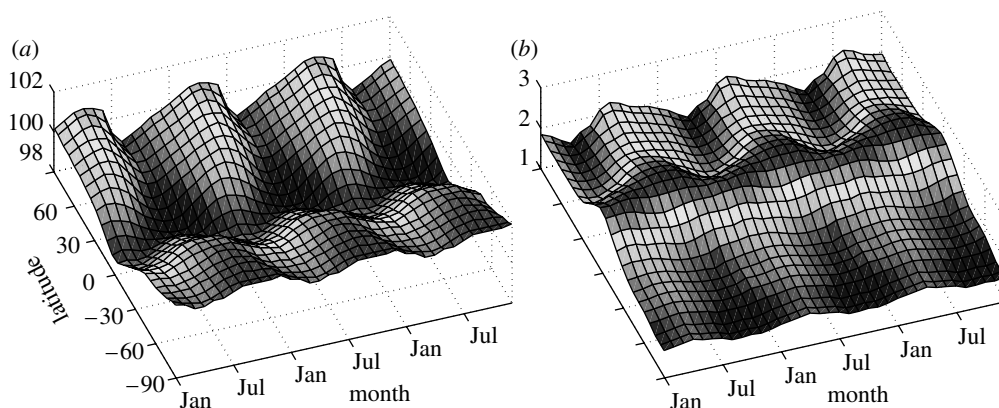
Figure 10. Zonal-mean, mid-tropospheric, seasonal patterns of (*a*) CH_4 (ppb) and (*b*) CO (ppb) in the primary, 14.2-yr mode of a three-dimensional global tropospheric chemistry–transport model with annually repeating meteorology. The e-fold of the perturbation has been removed to show the annually repeating patterns. The mode has been scaled to have an annual mean CH_4 perturbation of 100 ppb. Similar patterns (not shown) exist for O_3, NO_x and most other chemically reactive species.

Tropospheric chemistry in these CTMs has only one dominant long-lived mode. Once it has been characterized for a given atmospheric simulation, its properties can be used to extrapolate almost all perturbations based on that control simulation. (Long-lived gases such as CHF_2Cl that are present in very low abundances will also produce decadal modes, but with very small amplitudes.) Recognizing this, both Derwent *et al.* (2001) and Wild *et al.* (2001) studied a wide range of perturbations to short-lived species such as NO_x and CO. They calculated the long-term climate impacts from 4-yr CTM simulations by integrating the short-term changes in O_3 and then deriving the amplitude of the long-lived mode to explicitly integrate over the decadal changes in CH_4 and O_3.

11. Development and future directions

The chemical coupling between the stratosphere and the troposphere remains largely unexplored. Thus far, we have separately identified the CH_4-like tropospheric and N_2O-like stratospheric chemical modes. However, the CH_4-like mode will perturb stratospheric O_3 directly through reactions involving CH_4 and indirectly by increasing stratospheric H_2O. Changes in stratospheric O_3 will perturb N_2O and also tropospheric CH_4 chemistry through changing photolysis rates and OH. Lower-dimension models (e.g. §§3–9) may not accurately represent the stratosphere–troposphere coupling, but CTM studies of any chemical perturbation with an N_2O-like mode will need to integrate the perturbation-minus-control simulations for 50 yr or more to separate these two modes.

A practical breakthrough could be achieved if global atmospheric chemistry can be approximated by a finite Jacobian. For a reasonable number of degrees of freedom (e.g. 1000), the system can be solved for all eigenvectors. If such a matrix represented most of the important chemical modes, then it would provide an explicit model for following the response to perturbations to any

atmospheric species at any location. The challenge here is defining the space–time averaging kernels to reduce the dimensionality of the system while preserving the major modes.

One practical concern is whether the long-lived modes remain identifiable over the year-to-year variations in meteorology. Although different CTMs with different meteorological fields produce similar modes for stratospheric decay or tropospheric CH_4 chemistry, they are different enough to preclude ready evaluation of long-term impacts. Work with a single CTM and successive years of forecast meteorological fields is ongoing and should provide a quantitative measure of how the excitation and decay of chemical modes depend on meteorology. Similar questions arise regarding large year-to-year variations in atmospheric composition, such as for years with extensive forest fires.

Moving beyond atmospheric chemistry, extension of this approach to Earth system models could yield surprises. The coupling across different components of the chemistry–climate system, such as atmospheric chemistry, carbon cycle, marine biogeochemistry, aerosols and climate, may introduce new linkages and alter our expectation of the time scales of anthropogenic climate perturbations. Defining and computing these coupled chemistry–climate modes will be challenging.

References

Bolin, B. & Rodhe, H. 1973 Note on concepts of age distribution and transit-time in natural reservoirs. *Tellus* **25**, 58–62.

Bridgeman, C. H., Pyle, J. A. & Shallcross, D. E. 2000 A three-dimensional model calculation of the ozone depletion potential of 1-bromopropane (1-C_3H_7Br). *J. Geophys. Res.* **105**, 26 493–26 502. (doi:10.1029/2000JD900293)

Butler, J. H. 1994 The potential role of the ocean in regulating atmospheric CH_3Br. *Geophys. Res. Lett.* **21**, 185–188. (doi:10.1029/94GL00071)

Chapman, S. 1930 A theory of upper-atmosphere ozone. *Mem. R. Meteorol. Soc.* **3**, 103–125.

Church, J. A., White, N. J. & Arblaster, J. M. 2005 Significant decadal-scale impact of volcanic eruptions on sea level and ocean heat content. *Nature* **438**, 74–77. (doi:10.1038/nature04237)

Derwent, R. G., Collins, W. J., Johnson, C. E. & Stevenson, D. S. 2001 Transient behaviour of tropospheric ozone precursors in a global 3-D CTM and their indirect greenhouse effects. *Clim. Change* **49**, 463–487. (doi:10.1023/A:1010648913655)

Ehhalt, D. H., Rohrer, F., Schauffler, S. & Prather, M. 2004 On the decay of stratospheric pollutants: diagnosing the longest-lived eigenmode. *J. Geophys. Res.* **109**, D08 102. (doi:10.1029/2003JD004029)

Farrell, B. F. & Ioannou, P. J. 2000 Perturbation dynamics in atmospheric chemistry. *J. Geophys. Res.* **105**, 9303–9320. (doi:10.1029/1999JD901021)

Fisher, D. A. 1995 Calculated lifetimes and their uncertainties. In *Proc. Workshop on Atmospheric Degradation of HCFCs and HFCs, Boulder, CO, 17–19 November 1993*, pp. 1–5. Washington, DC: AFEAS Program Office section 3.

Hall, T. H. *et al.* 1999 Transport experiments. In *Models and measurements intercomparison II, Rep. NASA/TM-1999-20,9554* (eds J. H. Park *et al.*), ch. 2, pp. 110–189. Hampton, VA: NASA.

IPCC 1996 Climate change 1995. In *The science of climate change, Intergovernmental Panel on Climate Change* (eds J. T. Houghton *et al.*), p. 572. Cambridge, UK: Cambridge University Press.

Isaksen, I. S. A. & Hov, O. 1987 Calculation of trends in tropospheric O_3, OH, CH_4, and NOx. *Tellus B* **39**, 271–285.

Junge, C. E. 1974 Residence time and variability of tropospheric trace gases. *Tellus* **26**, 477.

Ko, M. K. W., Sze, N. D., Scott, C. J. & Weisenstein, D. K. 1997 On the relation between stratospheric chlorine/bromine loading and short-lived tropospheric source gases. *J. Geophys. Res.* **102**, 25 507–25 517. (doi:10.1029/97JD02431)

Manning, M. R. 1999 Characteristic modes of isotopic variations in atmospheric chemistry. *Geophys. Res. Lett.* **26**, 1263–1266. (doi:10.1029/1999GL900217)

Olsen, S. C., Hannegan, B. J., Zhu, X. & Prather, M. J. 2000 Evaluating ozone depletion from very short-lived halocarbons. *Geophys. Res. Lett.* **27**, 1475–1478. (doi:10.1029/1999GL011040)

O'Neill, B. C., Gaffin, S. R., Tubiello, F. N. & Oppenheimer, M. 1994 Reservoir timescales for anthropogenic CO_2 in the atmosphere. *Tellus-B* **46**, 378–389. (doi:10.1034/j.1600-0889.1994.t01-4-00004.x)

Prather, M. J. 1994 Lifetimes and eigenstates in atmospheric chemistry. *Geophys. Res. Lett.* **21**, 801–804. (doi:10.1029/94GL00840)

Prather, M. J. 1996 Time scales in atmospheric chemistry: theory, GWPs for CH_4 and CO, and runaway growth, Geophys. *Res. Lett.* **23**, 2597–2600. (doi:10.1029/96GL02371)

Prather, M. J. 1997 Timescales in atmospheric chemistry: CH_3Br, the ocean, and ozone depletion potentials. *Global Biogeochem. Cycles* **11**, 393–400. (doi:10.1029/97GB01055)

Prather, M. J. 1998 Time scales in atmospheric chemistry: coupled perturbations to N_2O, NOy, and O_3. *Science* **279**, 1339–1341. (doi:10.1126/science.279.5355.1339)

Prather, M. J. 2002 Lifetimes of atmospheric species: integrating environmental impacts. *Geophys. Res. Lett.* **29**, 2063. (doi:10.1029/2002GL016299)

Prather, M., Derwent, R., Ehhalt, D., Fraser, P., Sanhueza, E. & Zhou, X. 1995 Other tracer gases and atmospheric chemistry In *Climate change 1994, Intergovernmental Panel on Climate Change* (eds J. T. Houghton *et al.*), ch. 2, pp. 73–126. Cambridge, UK: Cambridge University Press.

Prather, M. *et al.* 2001 *Atmospheric chemistry and greenhouse gases* (eds J. T. Houghton *et al.*), ch. 4, pp. 239–287. Cambridge, UK: Cambridge University Press.

Ramaswamy, V., Boucher, O., Haigh, J., Hauglustaine, D., Haywood, J., Myhre, G., Nakajima, T., Shi, G. Y. & Solomon, S. 2001 Radiative forcing of climate change. In *Climate change 2001: the scientific basis* (eds J. T. Houghton *et al.*), ch. 6, pp. 349–416. Cambridge, UK: Cambridge University Press.

Solomon, S., Mills, M., Heidt, L. E., Pollock, W. H. & Tuck, A. F. 1992 On the evaluation of ozone depletion potentials. *J. Geophys. Res.* **97**, 825–842.

Waugh, D. W. & Hall, T. M. 2002 Age of stratospheric air: theory, observations, and models. *Rev. Geophys.* **40**, 1010. (doi:10.1029/2000RG000101)

Wild, O. & Prather, M. J. 2000 Excitation of the primary tropospheric chemical mode in a global three-dimensional model. *J. Geophys. Res.* **105**, 24 647–24 660. (doi:10.1029/2000JD900399)

Wild, O., Prather, M. J. & Akimoto, H. 2001 Indirect long-term global cooling from NOx emissions. *Geophys. Res. Lett.* **28**, 1719–1722. (doi:10.1029/2000GL012573)

WMO 1995 Scientific assessment of ozone depletion: 1994, global ozone research and monitoring project. Report no. 37, World Meteorological Organization, Geneva.

Wuebbles, D. J., Patten, K. O., Johnson, M. T. & Kotamarthi, R. 2001 New methodology for ozone depletion potentials of short-lived compounds: *n*-propyl bromide as an example. *J. Geophys. Res.* **106**, 14 551–14 571. (doi:10.1029/2001JD900008)